

## **Electronic Supplementary Information**

### **Preparation of graphene dispersions and graphene-polymer composites in organic media**

*Silvia Villar-Rodil, Juan. I. Paredes, Amelia Martínez-Alonso, Juan. M. D. Tascón*

Instituto Nacional del Carbón, CSIC, Apartado 73, 33080 Oviedo, Spain

### Experimental

Graphite oxide preparation, purification and drying were carried out as described in a previous paper.<sup>1</sup> For the preparation of graphene oxide dispersions in *N,N*-dimethylformamide (DMF) and *N*-methyl-2-pyrrolidone (NMP) with long-term stability, the dried product was first ground with mortar and pestle, and then added to the solvent and sonicated in an ultrasound bath cleaner (J.P. Selecta Ultrasons system, 40 kHz) for 2 h. The resulting dispersion was then centrifuged in an Eppendorf 5424 microcentrifuge at 10000 x g for 3 min to remove unexfoliated graphite oxide platelets, and the supernatant was collected and its concentration measured by UV-vis absorption. Conversion of the graphene oxide sheets dispersed in the organic solvents back to conducting graphene was carried out through reduction with *N,N*-dimethylhydrazine (DMH). Graphene oxide dispersions of known concentration (typically 0.1 mg mL<sup>-1</sup>, but working at higher concentrations, e.g. 0.3-0.4 mg mL<sup>-1</sup>, was also possible) were reacted with a given amount of DMH (1.3 mg of DMH per mg of graphene oxide) in a water bath at 95 °C for 1h, during which the light brown color of the unreduced dispersion turned completely black.

UV-vis absorption spectra of the dispersions were recorded in a double-beam He $\lambda$ ios  $\alpha$  spectrophotometer (Thermo Spectronic). The different samples of chemically reduced graphene were characterized by thermogravimetric analysis (TGA), Fourier transform infrared spectroscopy (FTIR), X-ray photoelectron spectroscopy (XPS), Raman spectroscopy and scanning tunneling microscopy (STM) after drying their corresponding organic dispersions. TGA was carried out in a SDT Q600 thermobalance (TA Instruments) under Ar gas flow (100 ml min<sup>-1</sup>) at a heating rate of 10 °C min<sup>-1</sup>. FTIR spectra were recorded in a Nicolet 8700 spectrometer (Thermo Scientific) using KBr pellets with a sample concentration of ~0.05 wt%. The recorded spectra were the result of coadding 64 interferograms obtained at a resolution of 4 cm<sup>-1</sup>. XPS measurements were made in a SPECS spectrometer under 10<sup>-7</sup> Pa with a monochromatic Al K $\alpha$  X-ray source using a power of 100 W. Raman spectra were recorded on a Jobin-Yvon LabRam instrument with laser excitation wavelength of 532 nm. STM imaging was accomplished under ambient conditions (relative humidity ~40%, temperature ~22-24 °C) with a Nanoscope IIIa Multimode apparatus (Veeco Instruments) operating in the constant current mode with tunneling parameters of 0.5 nA (tunneling current) and 500 mV (bias voltage). Mechanically prepared Pt/Ir (80/20) tips were employed. Samples for STM imaging were prepared by drop-casting a dilute dispersion of chemically reduced graphene oxide onto freshly cleaved, atomically flat highly oriented pyrolytic graphite (HOPG) and allowing it to dry in air at room temperature.

Graphene-polymer composite materials (1 wt% loading of graphene) were prepared by dissolving the polymer in a dispersion of chemically reduced graphene oxide in hot (~60° C) organic solvent and then coagulating the mixture in an appropriate solvent. Polyacrylonitrile (PAN) was solved in hot DMF dispersion of graphene nanosheets and the resulting blend was coagulated in water, whereas poly(methyl methacrylate) (PMMA) was dissolved in a hot dispersion in NMP and coagulated in methanol. Both mixtures were copiously washed with the coagulating solvents, allowed to dry in air and molded into pellets using a hydraulic press. Pure polymer pellets were also prepared for comparison. In the case of PAN, thin transparent films of pure polymer and graphene-polymer composite (~0.1 wt% loading of graphene) were also prepared by evaporation

---

(1) Paredes, J. I.; Villar-Rodil, S.; Martínez-Alonso, A.; Tascón, J. M. D. *Langmuir* **2008**, *24*, 10560.

of the organic solvent. The composites were examined by optical microscopy and, in the case of the PMMA-graphene composite, their thermal stability was studied with TGA.

### FTIR spectroscopy results

Fig. S1 shows the FTIR spectrum obtained for graphene oxide reduced in DMF together with that of graphite oxide to facilitate the comparison. The intensities of the bands assigned to oxygen functionalities in the graphite oxide material ( $3430\text{ cm}^{-1}$ , O-H stretching vibrations;  $1726\text{ cm}^{-1}$ , C=O stretching vibrations from carbonyl and carboxylic groups;  $1226\text{ cm}^{-1}$ , C-OH stretching vibrations; and  $1103\text{ cm}^{-1}$ , C-O stretching vibrations) strongly decrease upon reduction in relation to the intensity of the band assigned to the skeletal vibrations of graphitic domains ( $1588\text{ cm}^{-1}$ ).

### XPS spectroscopy results

XPS results confirm the reduction of graphene oxide. To start with, and unlike graphite oxide, no charge compensation is required for the reduced samples, as they are conductive enough not to become charged under the X rays. Furthermore, the decrease in oxygen functionalities is clear from the comparison of the C/O atomic ratios calculated from the survey spectra (not shown) of graphite oxide (atomic C/O=2.3)<sup>1</sup> to those calculated for reduced graphene oxide in DMF (7.0) and NMP (4.8). Some nitrogen (~2.7 at. %, for the sample produced in DMF) remains in the carbonaceous structure as a result of the treatment with DMH, as found in the literature for related materials obtained with a similar method.<sup>2,5</sup> In the case of the material reduced in NMP (nitrogen content of 5.9 at. %), nitrogen is introduced due both to the treatment with DMH and probably to the presence of residual solvent.<sup>6</sup> Regarding the high resolution C1s core level spectrum, reduction has had a great impact in the chemical environment of the carbon atoms, as the higher binding energy side of the C1s envelope, which constitutes the main feature for the unreduced material and stems from the most electropositive, oxidized carbons, decreases to yield just a tail after chemical reduction. In fact, the reduction has gone further than in most of the cases shown in the literature for similar materials.<sup>2,4,5,7-10</sup> The C1s band of graphite oxide (Fig. 2b, top) could be fitted to three components, located at 284.6 (FWHM=1.4 eV), 286.6 (FWHM=1.2 eV), and 287.9 eV (FWHM=2.0 eV). These components have been assigned to graphitic C-C, sp<sup>3</sup> C and C-O, and C=O species, respectively.<sup>11</sup> The C1s core level envelope of

---

(2) McAllister, M. J.; Li, J.-L.; Adamson, D. H.; Schniepp, H. C.; Abdala, A. A.; Liu, J.; Herrera-Alonso, M.; Milius, D. L.; Car, R.; Prud'homme, R. K.; Aksay, I. A. *Chem. Mater.* **2007**, *19*, 4396.

(3) Gómez-Navarro, C.; Weitz, R. T.; Bittner, A. M.; Scolari, M.; Mews, A.; Burghard, M.; Kern, K. *Nano Lett.* **2007**, *7*, 3499.

(4) Becerril, H. A.; Mao, J.; Stoltenberg, R. M.; Bao, Z.; Chen, Y. *ACS Nano.* **2008**, *3*, 463

(5) Park, S.; An, J.; Piner, R. D.; Jung, I.; Yang, D.; Velamakanni, A.; Nguyen, S. T.; Ruoff, R. S. *Chem. Mater.* **2008**, *20*, 6592.

(6) Hernandez, Y.; Nicolosi, V.; Lotya, M.; Blighe, F. M.; Sun, Z.; De, S.; McGovern, I. T.; Holland, B.; Byrne, M.; Gun'ko, Y. K.; Boland, J. J.; Niraj, P.; Duesberg, G.; Krishnamurthy, S.; Goodhue, R.; Hutchison, J.; Scardaci, V.; Ferrari, A. C.; Coleman, J. N. *Nature Nanotech.* **2008**, *3*, 563.

(7) Stankovich, S.; Dikin, D. A.; Dommett, G. H. B.; Kohlhaas, K. M.; Zimmey, E. J.; Stach, E. A.; Piner, R. D.; Nguyen, S. T.; Ruoff, R. S. *Nature* **2006**, *442*, 282.

(8) Fan, X.; Peng, W.; Li, Y.; Li, X.; Wang, S.; Zhang, G.; Zhang, F. *Adv. Mater.* **2008**, *20*, 4490.

(9) Stankovich, S.; Piner, R. D.; Chen, X.; Wu, N.; Nguyen, S. T.; Ruoff, R. *J. Mater. Chem.* **2006**, *16*, 155.

(10) Schniepp, H. C.; Li, J.-L.; McAllister, M. J.; Sai, H.; Herrera-Alonso, M.; Adamson, D. H.; Prud'homme, R. K.; Car, R.; Saville, D. A.; Aksay, I. A. *J. Phys. Chem. B* **2006**, *110*, 8535.

(11) Biniak, S.; Szymanski, G.; Siedlewski, J.; Swiatkowski, A. *Carbon* **1997**, *35*, 1799. Zhang, G.; Sun, S.; Yang, D.; Dodelet, J.-P.; Sacher, E. *Carbon* **2008**, *46*, 196.

chemically reduced graphene oxide (Fig. 2b, bottom) has been fitted to 5 components, whose maximum and structural assignments are the following:<sup>12</sup> 284.3 eV, extensively delocalized aromatic  $sp^2$  structures; 285.2 eV, localised aromatic  $sp^2$  structures; 286.2 eV,  $sp^3$  C and C-O and C-N single bonds; 287.7 eV,  $\pi \rightarrow \pi^*$  shake-up satellite of the  $sp^2$  band centred at 285.2 eV, and C=O bonds; 291.0 eV,  $\pi \rightarrow \pi^*$  shake-up satellite of the  $sp^2$  band centered at 284.3 eV. Upon reduction, the graphitic C-C band becomes narrower than that of graphite oxide (FWHM=0.9 eV), which suggests that a more homogeneous chemical environment and/or more ordered structure has been developed.

### Raman spectroscopy results

Fig. S2 shows Raman spectra of graphite oxide and graphene oxide reduced in DMF. The first order spectra (1100-1800  $cm^{-1}$ ) show the two well-known G and D bands characteristic of carbon materials. The G band, located at  $\sim 1590$   $cm^{-1}$ , corresponds to zone centre phonons of  $E_{2g}$  symmetry at the  $\Gamma$  point of the first Brillouin zone of graphite and involves in-plane bond stretching of  $sp^2$  carbon pairs. The D band located at  $\sim 1350$   $cm^{-1}$ , is assigned to K-point phonons of  $A_{1g}$  symmetry, only appears in disordered carbon materials and its intensity is connected to the presence of six-fold aromatic rings.<sup>13</sup> Thus, the ratio of the integrated intensities of the D and G bands ( $I_D/I_G$ ) is usually taken as an indication of the relative disorder present in graphitic structures. In the present case, chemical reduction of graphene oxide both in DMF and NMP (spectrum not shown to avoid repetition) brings about a decrease in  $I_D/I_G$ , (from 1.46 in graphite oxide to 1.37 and 1.32, respectively). Although such variations are not very significant, an increase (rather than a decrease) in  $I_D/I_G$  has been previously reported in the literature for related processes.<sup>2-14</sup> In principle, the latter would be an unexpected result, if taken as an indication of an increase of disorder. In fact, the changes introduced by chemical reduction in the Raman spectra of graphene oxide are not still well understood. In some cases, the increase in  $I_D/I_G$  after reduction of graphene oxide is explained as a result of a simultaneous increase in number and decrease in size of graphitic domains.<sup>15</sup> On the other hand, it has been recently suggested that unreduced graphene oxide is in an amorphous state and a graphite-like state is only recovered after reduction, implying that the  $I_D/I_G$  ratio cannot be directly compared between the two states.<sup>13,14</sup> The large amounts of hydroxyl and epoxy groups present in graphene can decrease the relative amount of six-fold aromatic rings, diminishing the intensity of the D band.<sup>13</sup> Such decrease in aromaticity agrees with the low electrical conductivity of unreduced graphene oxide. After chemical reduction, most of those oxygenated groups are eliminated, reintroducing aromaticity and electrical conductivity in the structure. If the reduction process is limited, the aromatic areas are small in size and thus the relative intensity of D band can rise, leading to the increase in  $I_D/I_G$ . If reduction is more extensive, as seems to have happened in our materials as compared with the ones in previous works in the literature, larger aromatic domains can be expected and the D band intensity can start to diminish, reflecting graphitic order. Anyway, the re-graphitization of the structure achieved by chemical reduction with DMH is at the best not complete and the reduced graphene oxide still possesses structural defects, which

---

(12) Zhang, G.; Sun, S.; Yang, D.; Dodelet, J.-P.; Sacher, E. *Carbon* **2008**, *46*, 196.

(13) Ferrari, A. C.; Robertson, J. *Phys. Rev. B* **2000**, *61*, 14095.

(14) Jung, I.; Dikin, D. A.; Piner, R. D.; Ruoff, R. S. *Nano Lett.* **2008**, *8*, 4283.

(15) Stankovich, S.; Dikin, D. A.; Piner, R. D.; Kohlhaas, K. M.; Kleinhammes, A.; Jia, Y.; Wu, Y.; Nguyen, S. T.; Ruoff, R. *Carbon* **2007**, *45*, 1558.

are clearly reflected in its Raman spectrum, totally different from that of pristine graphite.

#### **Additional details about STM and AFM measurements**

Fig. S3 shows additional representative nanometer-scale STM images of reduced graphene oxide. The tunneling conditions employed to study the reduced nanosheets (0.5 nA and 500 mV in the images, but working with higher currents and lower voltages was also possible) were those typically used for imaging well conductive carbon materials.<sup>16</sup> By contrast, the unreduced nanosheets could not be observed under similar tunneling conditions, which suggests that they are not electrically conductive, as expected. Most probably, the unreduced nanosheets are swept away by the STM tip, so that only the pristine HOPG substrate can be visualized, as it was indeed the case. STM results obtained for the reduced graphene oxide nanosheets were further checked with the use of atomic force microscopy (AFM), which again revealed the presence of sheets with uniform thickness (~1 nm). The AFM-derived thickness agrees with that reported previously for graphene oxide nanosheets reduced in water,<sup>17</sup> but is slightly larger than that derived by STM. This result can be attributed to the fact that the thickness measured by these techniques is influenced by the imaging mechanism, which introduces an instrumental offset in the measurement. As the imaging mechanism in STM is very different to that of AFM, different offsets, and therefore somewhat different measured thicknesses, should be expected. We also note from the line profiles that the nanosheets are not flat, but atomically rough, even though the substrate (HOPG) is atomically flat. Such observation can be attributed to structural distortions in the carbon skeleton of the reduced nanosheets, such as point or line defects (see Raman spectroscopy data, Fig. S2), that lead to wrinkling on the atomic scale.<sup>3</sup> Taken together, the STM observations indicate that reduction in the organic solvents was successful (electrical conductivity was restored) and that the graphene oxide nanosheets remained in these solvents as individual, single-layer objects after reduction. Such result is significant, as it implies that individual, single-layer graphene nanosheets in the form of chemically reduced graphene oxide can be easily prepared in organic media, and thus not only in water, without the need of functionalizing the nanosheets, thus facilitating their practical use.

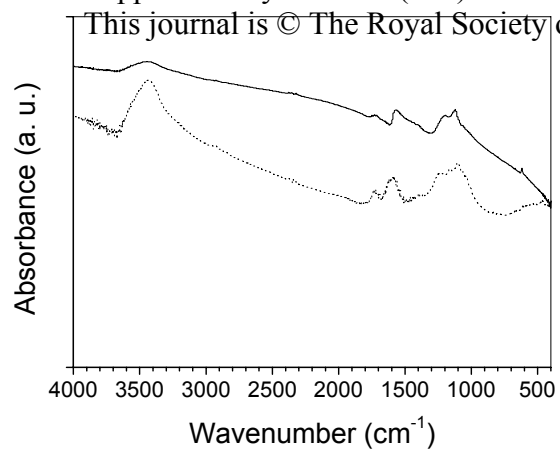
#### **Graphene-PAN composite**

Fig. S4 shows pellets and films of pure PAN and graphene-PAN composite. As can be seen, graphene imparts black color to the composite pellets, while the graphene-PAN composite film is transparent and grey. The composite displays a homogeneous appearance both by visual inspection (see digital picture in Fig. S4a) and in the micrometer range (see optical microscopy image in Fig S4c).

---

(16) Paredes, J. I.; Martínez-Alonso, A.; Tascón, J. M. D. *Langmuir* **2007**, *23*, 8932.

(17) Li, D.; Müller, M. B.; Gilje, S.; Kaner, R. B.; Wallace, G. G. *Nature Nanotech.* **2008**, *3*, 101.



**Figure S1.** FTIR spectra of chemically reduced graphene oxide in DMF (solid line) and graphite oxide (dotted line).

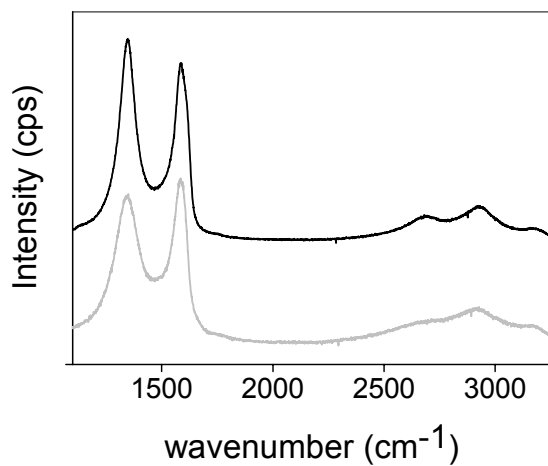


**Figure S2.** Raman spectra of graphite oxide (grey) and graphene oxide reduced in DMF (black).

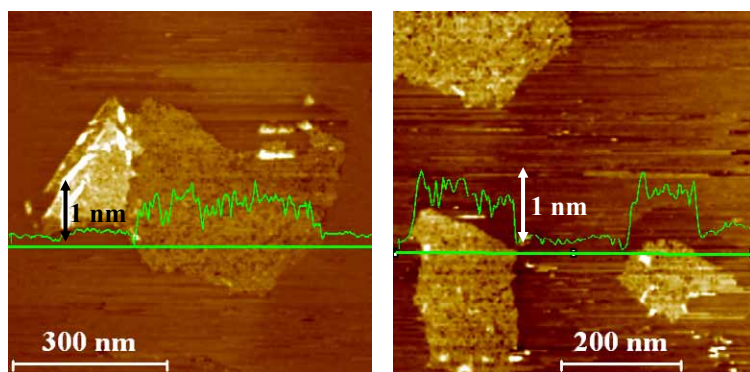


**Figure S3.** Typical nanometer-scale STM images of reduced graphene oxide on HOPG with overlapping line profiles along the lines indicated. The up-down arrows indicate the height of the reduced graphene oxide sheets.



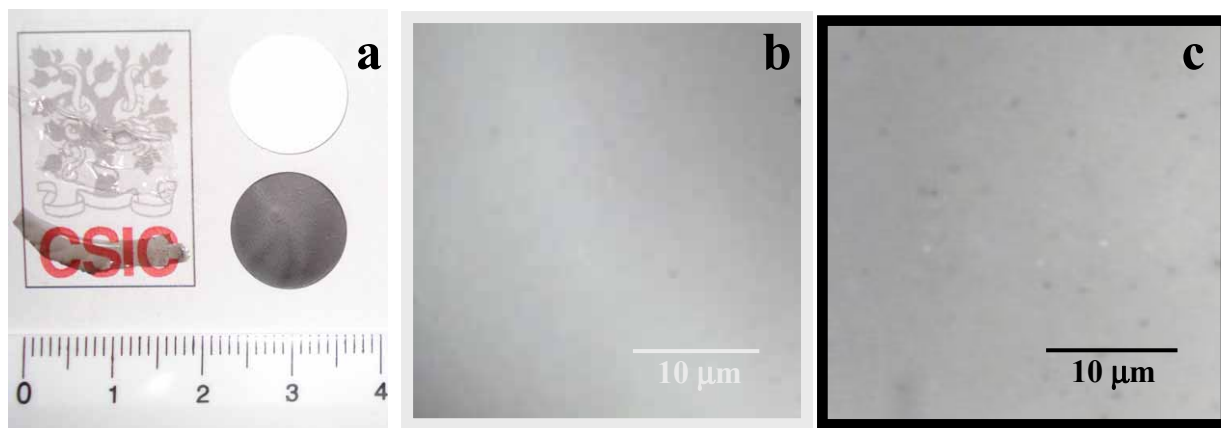


**Fig. S4.** (a) Digital photograph of PAN (top) and a composite of PAN with graphene oxide reduced in DMF (bottom) both as thin transparent films (left) and as pellets (right). Pure PAN film has been surrounded by a white square to facilitate its location. (b) Typical optical microscopy images of pure PAN film (top left) and (c) reduced graphene oxide-PAN composite film (bottom left).